Available online at www.sciencedirect.com

ScienceDirect

Procedia Engineering 126 (2015) 617 – 621

Procedia Engineering

www.elsevier.com/locate/procedia

7th International Conference on Fluid Mechanics, ICFM7

Numerical study of shock/boundary layer interaction of chemically reacting flow in shock tube

Song Chen, Quanhua Sun*

State Key Laboratory of High Temperature Gas Dynamics, Institute of Mechanics, Chinese Academy of Sciences, 100190 Beijing, China

Abstract

In this paper, a high-order Navier-Stokes solver is developed for chemically reacting flow and is applied to investigate the unsteady, viscous interaction between shock wave and boundary layer in an air filled shock tube. The solver employs a high-resolution weighted essentially non-oscillatory (WENO) scheme to capture the complex flow pattern induced by shock/boundary-layer interaction, together with a point-implicit method to overcome the stiffness of chemical production term. The results show the influence of real gas effects and give insights into the mechanism of shock/boundary-layer interaction process.

Peer-review under responsibility of The Chinese Society of Theoretical and Applied Mechanics (CSTAM)

Keywords: Shock/boundary-layer interaction; Nonequilibrium chemical reactions; Shock tube flow; WENO scheme.

1. Introduction

The interaction of shock wave and boundary layer is a classic problem in gas dynamics. The interaction creates complex flow pattern in shock tube when a shock is reflected from the end-wall although the setup is quite simple. It is still a challenging task for numerical simulation to capture the details of this problem.

Weber [1] made an early numerical study of two dimensional viscous flow in a shock tube using a flux-corrected transport algorithm. He investigated the influence of Reynolds number, Mach number and wall temperature on the shock bifurcation process. However, his computation domain only contains the region near the end wall, thus contact surface and rarefaction waves were excluded from the simulation. Sjogreen & Yee [2] later performed a more strict numerical investigation about the unsteady shock tube problem and concluded that an extreme grid refinement and time step restrictions were needed to resolve all the flow scales as well as the chemical reaction scales. This conclusion implies that it is quite difficult to obtain sufficiently accurate numerical results with acceptable computational cost. Daru & Tenaud [3], who carried out a careful study of this problem by using a high-order resolution monotonicity-preserving scheme (OSMP7), presented grid converged results for perfect gas flow of Reynolds number in the range 200 ~ 1000. Although there are some high-order simulation results of viscous shock tube problem recently, detailed analysis with respect to the interaction mechanism as well as the flow dynamics is seldom reported in the literature.

* Quanhua Sun. Tel.: +86-10-82544023.
E-mail address: qsun@imech.ac.cn

Peer-review under responsibility of The Chinese Society of Theoretical and Applied Mechanics (CSTAM)
doi:10.1016/j.proeng.2015.11.249

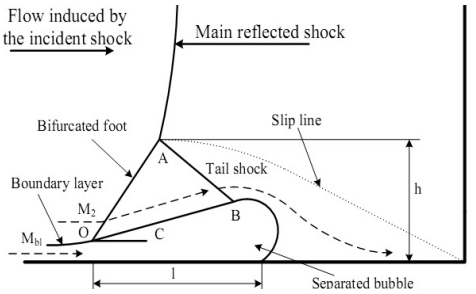

Fig. 1. Schematic of shock wave and boundary layer interaction.

In the present study, we firstly develop a high-order Navier-Stokes solver for chemically reacting flow. After verified with several test cases, the solver is applied to study a two-dimensional, unsteady, viscous shock tube flow that is sketched in Fig. 1. The details are presented in the following sections.

2. Numerical procedures

The 2D Navier-Stokes equations for chemically reacting flow can be expressed as follows

$$\frac{\partial \mathbf{U}}{\partial t} + \frac{\partial \mathbf{F}}{\partial x} + \frac{\partial \mathbf{G}}{\partial y} = \frac{\partial \mathbf{F}_v}{\partial x} + \frac{\partial \mathbf{G}_v}{\partial y} + \mathbf{S}, \tag{1}$$

where $\mathbf{U}$ is the solution vector of the conservative variables, $\mathbf{S}$ is the chemical source term, $\mathbf{F}, \mathbf{G}$ and $\mathbf{F}_v, \mathbf{G}_v$ are the inviscid and viscous fluxes respectively. The viscosity of each species in air is calculated using a curve fit function, and the mixture viscosity is evaluated using the Wilke's law. The thermal conductivity is obtained via a constant Prandtl number (Pr=0.73). The Fick's law is assumed for mass diffusion, and the Schmidt number is fixed at 0.5. The chemical reaction rates are modelled using the Arrhenius expressions. Detailed expressions can be found in Ref. [4].

The inviscid fluxes are approximated using the WENO scheme of Jiang & Shu [5]. In this work, we use the five-point stencil and thus five order is obtained for the inviscid fluxes. A local Lax-Friedrichs flux-vector splitting technique is applied for the identification of the upwind direction

$$\triangle \mathbf{F}^{m\pm}_{i+1/2} = \triangle \mathbf{F}^{m\pm}_{i+1} + \triangle \mathbf{F}^{m\pm}_{i}, \qquad \triangle \mathbf{F}^{m\pm}_{i} = 0.5\left(\triangle \mathbf{F}^{m\pm}_{i} \pm \Lambda^{m}_{i,max}\mathbf{U}_i\right), \tag{2}$$

where $\Lambda^{m}_{i,max}$ is the mth maximum eigenvalue of the flux Jacobian inside the stencil. The viscous fluxes are discretized by means of a six-order accurate central scheme. A point-implicit method is employed to incorporate the advantages of implicit integration with respect to the chemical source term into an explicit method, in which the source term $\mathbf{S}(\mathbf{U}^{n+1})$ is obtained using the first order Taylor expansion

$$\mathbf{S}(\mathbf{U}^{n+1}) = \mathbf{S}(\mathbf{U}^{n}) + \frac{\partial \mathbf{S}}{\partial \mathbf{U}}\triangle \mathbf{U} + O(\triangle \mathbf{U}^2), \tag{3}$$

Together with the 3-stage Runge-Kutta formula, the scheme can be written as

$$\left[\mathbf{I} - \alpha_k \triangle t \frac{\partial \mathbf{S}}{\partial \mathbf{U}}\right]\triangle \mathbf{U}_k = (1-\alpha_k)(\mathbf{U}^n - \mathbf{U}_{k-1}) + \alpha_k \triangle t\left[-\frac{\partial \mathbf{F}}{\partial x} + \mathbf{S}(\mathbf{U}^n)\right], \tag{4}$$

where $\mathbf{I}$ is the unit matrix, and subscript $k = \{1, 2, 3\}$ denotes the kth step of Runge-Kutta loops. Thus, $\triangle \mathbf{U}_1 = \mathbf{U}_1 - \mathbf{U}^n$, $\triangle \mathbf{U}_2 = \mathbf{U}_2 - \mathbf{U}_1$, $\triangle \mathbf{U}_3 = \mathbf{U}^{n+1} - \mathbf{U}_2$. The coefficients $\alpha_k = \{1, 1/4, 2/3\}$. Since $\alpha_1 = 1$, the first term in the right-hand side will vanish at the first step. $\mathbf{U}_1$ and $\mathbf{U}_2$ are the intermediate solutions of Runge-kutta steps. If the coefficient of $\partial \mathbf{S}/\partial \mathbf{U}$ is set to zero, Eq.(4) will reduce to the explicit Runge-Kutta scheme.

The problem now is transformed to the classic matrix equation $\mathbf{AX} = \mathbf{B}$. Here $\mathbf{X}$ represents $\triangle \mathbf{U}_k$, $\mathbf{A}$ represents the coefficient matrix, and $\mathbf{B}$ represents the right-hand side terms. A *gaussian elimination with pivoting algorithm* method is employed to solve the matrix equation at each Runge-Kutta step.

3. Verification

The numerical method is implemented in a framework of Navier-Stokes solver. The code is fully parallelized using MPI-libraries and has been verified using several test cases.

The first test case is to simulate an acoustic wave travelling across a periodic domain of length L_{x_1}=5 mm in a pure oxidizer mixture, which was previously studied by Vicquelin et al. [6] and re-examined recently by Martinez Ferrer et al. [7]. The current aim is to verify the performance of the WENO scheme when coupled with multicomponent diffusive terms. Figure 2(a) is the temperature evolution at x_1^*=0, which shows good agreement between the present results and those of Vicquelin et al.

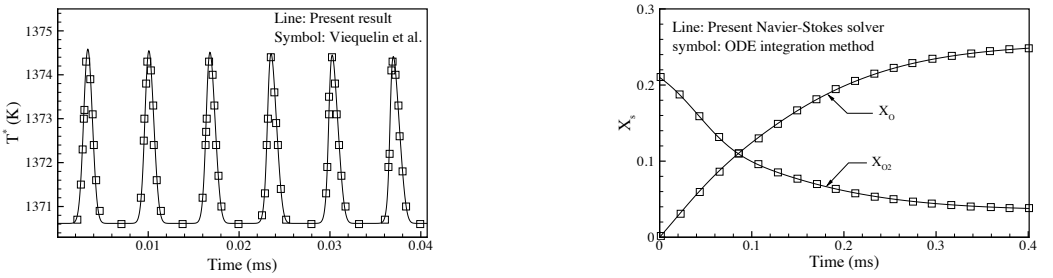

(a) Time evolution of the temperature. (b) X_{O2} and X_O variation

Fig. 2. Test case: (a) Propagation of an acoustic wave; (b) Perfectly stirred reactor under p=1.0 atm and T=4000K.

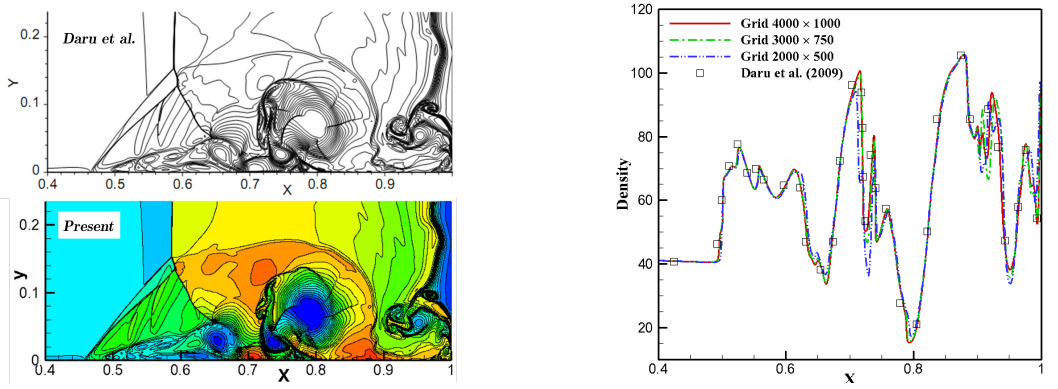

(a) Density field comparison. (b) Distributions of density along the line y=0.05.

Fig. 3. Two-dimensional shock tube verification case.

The second case is concentrated on the verification of chemical production term. We consider the evolution of a constant volume of air, which is instantaneously heated to a temperature of 4000 K under 1.0 atm pressure. The mixture is modelled with five species, namely O_2, O, N_2, N and NO. The calculated time histories of mole fractions, X_{O2} and X_O, are compared to the results obtained using the Selected Asymptotic Integration Method (SAIM) method reported in Ref. [1]. As shown in Fig. 2(b), the numerical solutions are in excellent agreement with results obtained using the SAIM method.

The 2D shock/boundary layer interaction of a perfect gas, which was studied previously by Daru & Tenaud [3], is used as the last case for the purpose of assessing complex flow simulations. Figure 3(a) shows the density field at dimensionless time $t = 1$, and Fig. 3(b) is the density distribution along the horizontal line crossing the separation bubble located at $y = 0.05$. These results demonstrate that the present solver is able to capture complex vortex structure and the grid converged solution is the same as that predicted by Daru & Tenaud.

4. Analysis of shock/boundary-layer interaction in shock tube

In this section, the two-dimensional case of Daru & Tenaud is revisited for chemically reacting air. The computational domain contains the region of (x=0~1 m, y=0~0.25 m), which could represents the flow in the middle cross section of a rectangle shock tube. The corner effects due to the side wall of a real shock tube are considered small compared to those of other factors in present study. The diaphragm is initially located at the middle of the tube. Both sections contain air, initially in chemical equilibrium. Since high Reynolds number flows require finer grids to achieve grid convergence, the initial pressures are setted at P_L=12 kPa and P_R=0.12 kPa to keep a low Reynolds number. The initial temperature is 800 K for both sections. In order to reduce the computational cost and show the dissociation effect, the air is modelled using three species, i.e., O_2, O and N_2, which is valid when the flow temperature is not very high (T <~ 4000 K). The computations were carried out on a parallel computer using 128 processors. Selected results (nondimensionlized by initial value of left section) are presented below to show the physics of the problem.

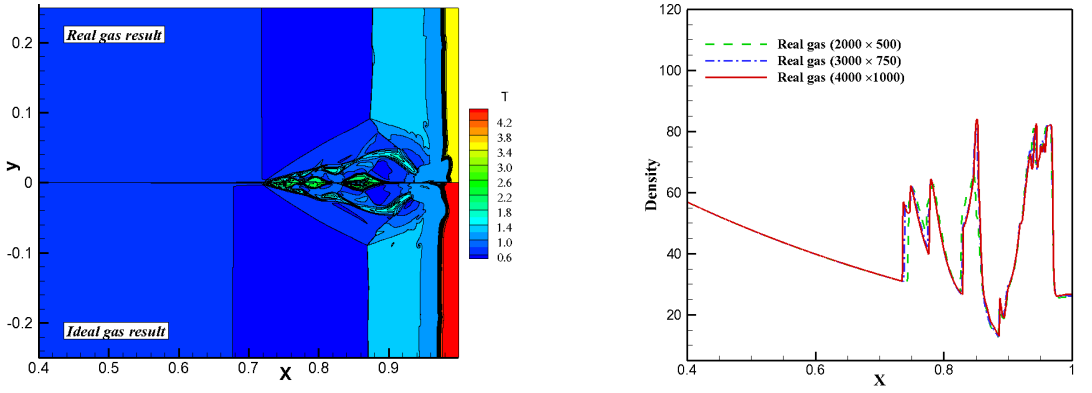

(a) Temperature field comparison. (b) Distributions of density along the line y=0.05.

Fig. 4. The simulation results for 2D viscous shock tube flow with real gas effects.

Figure 4(a) compares the temperature field between the ideal and real gas cases. Because of the real gas effects due to vibrational excitation and chemical reaction, the temperature in region 5 of shock tube is significantly reduced. The highest temperature, is only about 2900 K in the real gas case as compared with 3600 K in the ideal gas case. It should be mentioned that the flow pattern is not greatly changed with real gas effects. Figure 4(b) plots the density distribution along$y$ = 0.05, which shows clearly that grid converged solutions are obtained.

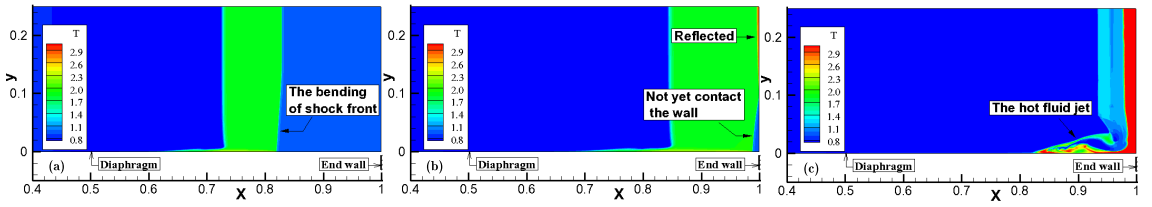

Fig. 5. Temperature field at time step of (a) nstep=3150, (b)nstep=4800 and (c) nstep=9600.

For the shock wave/boundary-layer interaction, it is generally stated that the boundary layer does not have sufficient energy to penetrate the reflected shock region, and begins to stagnate. This process together with the interaction of the attendant compression waves with the reflected shock near the wall cause to form a triple shock structure [1]. Our simulation results reveal detailed mechanism of the shock/boundary-layer interaction process, which can be illustrated using Fig. 5 and 6. After the diaphragm breaks up, a shock front is formed immediately and starts to move forward. The shock, however, will bend near the surface of shock tube due to the viscous effects. As the shock front approaches the end-wall, the curved shape becomes more apparent. This behaviour leads to a reflection that is actually out of sync

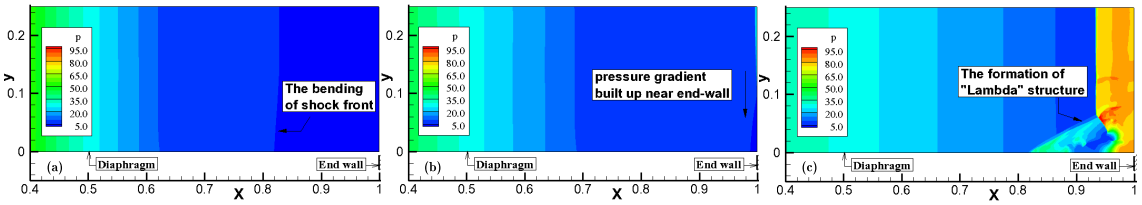

Fig. 6. Pressure field at time step of (a) nstep=3150, (b)nstep=4800 and (c) nstep=9600.

at the end-wall. Namely, when the core part of shock front is reflected, the shock front near the wall may still not touch the end-wall. Therefore, a strong pressure gradient is established in the vertical direction, which pushes the flow to the corner. The flow then recirculates and rolls up at the corner, eventually forms a ”bubble” and forms the lambda-shape shock structure.

5. Concluding remark

A high-order Navier-Stokes solver for reacting flow has been developed and verified in this work. Comparisons between present results and solutions in the references are satisfactory. With the developed solver, a careful numerical study is made to the two-dimensional viscous shock tube problem. Grid convergent results are obtained and exhibit significant difference in temperature to that obtained using ideal gas model. It is observed that the shock front bends near the surface of shock tube due to viscous effects, causing a successively contact and reflection of the shock front at different position of the end-wall. This process generates a vertical pressure gradient near the end-wall, which contributes to the formation of the lambda-shape structure during the shock wave/boundary-layer interaction.

The present investigation, however, is limited to the two-dimensional symmetric shock tube. For real shock tubes having a spanwise dimension of the same order as the bifurcation height, the corner effects could become important. Thus, future work of careful three-dimensional simulations are expected and may acquire a deeper understanding about the shock/boundary-layer interaction phenomena.

Acknowledgements

This work was supported by the National Natural Science Foundation of China through grants 11372325 and 91116013. Part of the work was completed in the shock wave laboratory of RWTH Aachen University. The authors are indebted to Prof. Olivier and Prof. Klioutchnikov for providing necessary facilities and constructive comments.

References

[1] Y.S.Weber, The numerical simulation of the reflected-shock/boundary-layer interaction in shock tubes, Ph.D. thesis, University of the Maryland College Park, 1994.
[2] B.Sjogreen, H.C.Yee, Grid convergence of high order methods for multiscale complex unsteady viscous compressible flows, J. Comput. Phys 185 (2003) 1–26.
[3] V.Daru, C.Tenaud, Numerical simulation of the viscous shock tube problem by using a high resolution monotonicity-preserving scheme, Comput. Fluids 38 (2009) 664–675.
[4] J.D.Anderson, Hypersonic and high temperature gas dynamics (2nd ed), AIAA Inc., Virginia, 2006.
[5] G.S.Jiang, C.W.Shu, Efficient implementation of weighted eno schemes, J. Comput. Phys 126 (1996) 202–28.
[6] R.Vicquelin, et al., Coupling tabulated chemistry with compressible cfd solvers, Proc. Combust. Inst. 33 (2011) 1481–1488.
[7] P. J.M.Ferrer, et al., A detailed verification procedure for compressible reactive multicomponent navierstokes solvers, Comput. Fluids 89 (2014) 88–110.